


Synthesis and evaluation of copper(II) complexes with isoniazid-derived hydrazones as anticancer and antitubercular agents

Gisele S. S. Firmino · Marcus V. N. de Souza · Claudia Pessoa ·
Maria C. S. Lourenco · Jackson A. L. C. Resende · Josane A. Lessa 

Received: 26 August 2016 / Accepted: 28 August 2016 / Published online: 3 September 2016
© Springer Science+Business Media New York 2016

Abstract In this study, the *N,N,O* metal chelator 2-pyridinecarboxaldehydeisonicotinoyl hydrazone (HPC IH, **1**) and its derivatives 2-acetylpyridine-(HAPIH **2**), 2-pyridineformamide-(HPAmIH, **3**) and pyrazineformamide-(HPzAmIH, **4**) were employed in the synthesis of four copper(II) complexes, [Cu(HPCIH)Cl₂].0.4H₂O (**5**), [Cu(HAPIH)Cl₂].1.25H₂O (**6**), [Cu(HPAmIH)Cl₂].H₂O (**7**) and [Cu(HPzAmIH)Cl₂].1.25H₂O (**8**). The compounds were assayed for their action toward *Mycobacterium tuberculosis* H37Rv ATCC 27294 strain and the human tumor cell lines OVCAR-8 (ovarian cancer), SF-295 (glioblastoma multiforme) and HCT-116 (colon adenocarcinoma). All copper(II) complexes were more effective in reducing growth of HCT-116 and SF-295 cells

than the respective free hydrazones at 5 µg/mL, whereas only complex **7** was more cytotoxic toward OVCAR-8 lines than its ligand HPAmIH. **6** proved to be cytotoxic at submicromolar doses, whose IC₅₀ values (0.39–0.86 µM) are similar to those ones found for doxorubicin (0.23–0.43 µM). Complexes **5** and **6** displayed high activity against *M. tuberculosis* (MIC = 0.85 and 1.58 µM, respectively), as compared with isoniazid (MIC = 2.27 µM), which suggests the compounds are attractive candidates as antitubercular drugs.

Keywords Copper(II) complexes · Hydrazones · Isoniazid · Anticancer agent · Antitubercular agent

Electronic supplementary material The online version of this article (doi:10.1007/s10534-016-9968-7) contains supplementary material, which is available to authorized users.

G. S. S. Firmino · J. A. Lessa (✉)
Departamento de Química Geral e Inorgânica, Instituto de
Química, Universidade do Estado do Rio de Janeiro-
UERJ, Rio de Janeiro, RJ 20550-900, Brazil
e-mail: josane@uerj.br

M. V. N. de Souza
Instituto de Tecnologia em Fármacos-Farmanguinhos,
Fundação Oswaldo Cruz-FioCruz, Rio de Janeiro,
RJ 21041-250, Brazil

C. Pessoa
Laboratório de Oncologia Experimental, Universidade
Federal do Ceará-UFC, Fortaleza, CE 60430-270, Brazil

M. C. S. Lourenco
Instituto Nacional de Infectologia Evandro Chagas,
Fundação Oswaldo Cruz-FioCruz, Rio de Janeiro,
RJ 21040-360, Brazil

J. A. L. C. Resende
Instituto de Química, Universidade Federal Fluminense-
UFF, Niterói, RJ 24020-141, Brazil

J. A. L. C. Resende
Instituto de Ciências Exatas e da Terra, Centro
Universitário do Araguaia, Universidade Federal do Mato
Grosso, Barra do Garças, MT 786000-000, Brazil

Introduction

Isoniazid (INH) was first introduced in tuberculosis therapy in the 1950s (Judge et al. 2012). Since then, it is regarded as one of the most commonly used and efficient drugs in treatment of human tuberculosis (Bernardes-Génisson et al. 2013).

In spite of efforts to eradicate tuberculosis, its burden remains substantial (Dheda et al. 2016). Over one-third of the global population is infected by tuberculosis, which causes death in approximately two to three million people annually (WHO 2014). The increased incidence of multidrug-resistant (Prozorov et al. 2012), and more recently, extensively drug-resistant (Sotgiu et al. 2009) strains of *Mycobacterium tuberculosis* compromise the recurrent effective treatment and evidences the urgency for novel antituberculosis agents (Hoagland et al. 2016).

Modification of existing drugs and the development of novel active compounds have been some of the strategies to improve tuberculosis drug therapy (Wong et al. 2013; Ellis et al. 2014; Chaves et al. 2015). In this sense, INH has become the most researched antitubercular agent (Hearn et al. 2009). A range of isoniazid analogues has been studied for its antitubercular potential and a number of promising candidates has been described (Oludina et al. 2014; Parumasivam et al. 2013; Matei et al. 2013; Ramani et al. 2012; Kumar et al. 2014).

Recently, Ellis and co-workers (2014) noticed that the INH analogue 2-pyridinecarboxaldehyde isonicotinoyl hydrazone (HPCIH), an effective iron chelator, displays potent inhibition of mycobacterial growth, probably acting as a lipophilic vehicle for the transport of the intact INH moiety into the mycobacterium. In spite of its marked antimycobacterial action, it has been shown HPCIH presents limited antiproliferative activity against malignant SK-N-MC (neuroepithelioma) (Becker and Richardson 1999). In our previous work, we demonstrated the analogues 2-acetylpyridine-(HAPIH), 2-benzoylpyridine-(HBPIH), 2-pyridineformamide-(HPAmIH) and 2-pyrazineformamide-(HPzAmIH) isonicotinoyl hydrazones in general exhibit better growth-inhibiting properties towards MCF-7, OVCAR-8 and SF-295 cells than HPCIH (Amim et al. 2016).

Metal complexes of substituted hydrazones have been reported to hold therapeutic activity and have shown pharmacological applications (Lessa et al. 2012, 2013; Raman et al. 2008; Chang et al. 2015).

It has been evidenced that the presence of an $\alpha(N)$ heterocyclic ring at azomethine scaffold of hydrazones plays a major role in extending their chelating and/or pharmacological properties (Beraldo and Gambino 2004).

Due to the effectiveness of HPCIH (Armstrong et al. 2003) and its analogues (Ababei et al. 2010; Chang et al. 2015) as tridentate chelating agents for transition metal ions, in this work we report the synthesis of four copper(II) complexes (**5–8**) with HPCIH (**1**), HAPIH (**2**), HPAmIH (**3**) and HPzAmIH (**4**) (Fig. 1). As part of our interest in the development of copper(II) complexes as antimycobacterial and anticancer agents, compounds **5–8** were assayed for their action toward *Mycobacterium tuberculosis* H37Rv ATCC 27294 strain and the human tumor cell lines OVCAR-8 (ovarian cancer), SF-295 (glioblastoma multiforme) and HCT-116 (colon adenocarcinoma).

Materials and methods

Chemicals

Isoniazid, 2-pyridinecarboxaldehyde, 2-acetylpyridine, 2-pyridinecarbonitrile, pyrazinecarbonitrile and copper(II) chloride dihydrate were purchased from Aldrich and used without further purification.

Physical measurements

Partial elemental analyses were performed on a Perkin Elmer CHN 2400 analyzer. Melting points were determined on Gehaka-PF1500 Farma, a Capillary Melting Point Apparatus. A CG 1800 Gehaka conductivity bridge (conductometric cell constant 1 cm^{-1}) was employed for molar conductivity measurements of compound solutions ($1 \times 10^{-3} \text{ mol L}^{-1}$) in dimethylsulfoxide (DMSO). Infrared spectra were recorded on an attenuated total reflectance/Fourier transform infrared spectrometer (Varian FT-IR 660) in the $4000\text{--}600 \text{ cm}^{-1}$ range. Electronic spectra were recorded on an Agilent Technologies 8453 spectrophotometer at room temperature, using a 10 mm beam path quartz cuvette and DMSO as solvent. Magnetic susceptibility measurements were carried out at $298.5 \text{ }^\circ\text{C}$ on a Johnson Matthey MSB/AUTO balance.

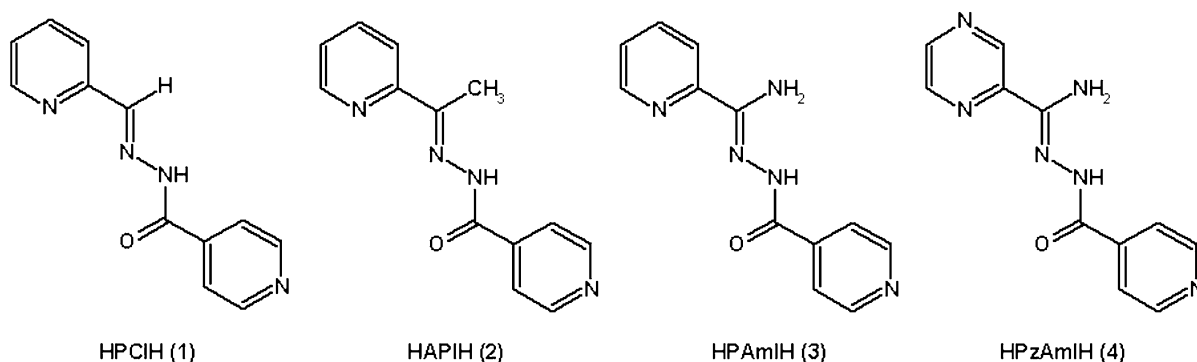


Fig. 1 Structures of $\alpha(N)$ heterocyclic isoniazid-derived hydrazones HPCIH (1), HAPIH (2), (HPAmIH) (3) and HPzAmIH (4)

Synthesis of the hydrazones (1–4) and their copper(II) complexes (5–8)

Synthesis of HPCIH (1) (Armstrong et al. 2003), HAPIH (2) (Ababei et al. 2010), HPAmIH (3) (Amim et al. 2016), and HPzAmIH (4) (Glushkov et al. 2004) are described in the literature. Copper(II) complexes 5–8 were obtained by mixing, under reflux and stirring for 4 h, a methanol solution (15 mL) of the desired hydrazone (1 mmol) with $\text{CuCl}_2 \cdot 2\text{H}_2\text{O}$ in 1:1 ligand-to-metal molar ratio. The resulting solids were filtered off, then washed with methanol followed by diethylether and dried at 50 °C for 24 h. Single crystals of $[\text{Cu}(\text{HAPIH})\text{Cl}]\text{Cl} \cdot \text{H}_2\text{O}$ (6a) and $[\text{Cu}(\text{HPzAmIH})\text{Cl}_2] \cdot \text{H}_2\text{O}$ (8a) were obtained from mother solutions of 6 and 8, respectively.

Dichloro(2-pyridinecarboxaldehyde-isonicotinoyl hydrazone)copper(II)] hydrate, $[\text{Cu}(\text{HPCIH})\text{Cl}_2] \cdot 0.4\text{H}_2\text{O}$ (5)

Green solid. Anal. Calc. for $\text{C}_{12}\text{H}_{10.8}\text{Cl}_2\text{CuN}_4\text{O}_{1.4}$ (FW = 367.89 g mol⁻¹): C, 39.18; H, 2.96; N, 15.23. Found: C, 39.50; H, 2.79; N, 14.76 %. IR (ATR, cm⁻¹): $\nu(\text{N}_{\text{py}}^+-\text{H})$ 2555, $\nu(\text{C}=\text{N})$ 1523, $\rho(\text{py})$ 644. Molar conductivity (1×10^{-3} mol L⁻¹, DMSO) 46.0 Ω^{-1} cm² mol⁻¹. Effective magnetic moment: 1.91 MB. UV–vis (DMSO, λ in nm/ ϵ in mol⁻¹dm²): 386/3.02 $\times 10^5$, 752/521. Yield 42 %.

Dichloro(2-acetylpyridine-isonicotinoyl hydrazone)copper(II) hydrate, $[\text{Cu}(\text{HAPIH})\text{Cl}_2] \cdot 1.25\text{H}_2\text{O}$ (6)

Green solid. Anal. Calc. for $\text{C}_{13}\text{H}_{14.5}\text{Cl}_2\text{N}_4\text{O}_{2.25}\text{Cu}$ (FW = 397.23 g mol⁻¹): C, 39.31; H, 3.68; N, 14.10 %. Found: C, 39.47; H, 3.43; N, 13.82 %. IR (ATR, cm⁻¹): $\nu(\text{N}_{\text{py}}^+-\text{H})$ 2569, $\nu(\text{C}=\text{N})$ 1531, $\rho(\text{py})$

645. Molar conductivity (1×10^{-3} mol L⁻¹, DMSO): 33.4 Ω^{-1} cm² mol⁻¹. Effective magnetic moment: 1.85 MB. UV–vis (DMSO, λ in nm/ ϵ in mol⁻¹dm²): 383/1.34 $\times 10^5$; 743/136. Yield 77 %.

Dichloro(2-pyridineformamide-isonicotinoyl hydrazone)copper(II) hydrate, $[\text{Cu}(\text{HPAmIH})\text{Cl}_2] \cdot \text{H}_2\text{O}$ (7)

Brown solid. Anal. Calc. for $\text{C}_{12}\text{H}_{13}\text{Cl}_2\text{CuN}_5\text{O}_2$ (FW = 393.71 g mol⁻¹): C, 36.61; H, 3.33; N, 17.79 %. Found: C, 36.65; H, 2.85; N, 17.33 %. IR (ATR, cm⁻¹): $\nu(\text{N}-\text{H})$ 3064, $\delta(\text{NH}_2)$ 1658, $\nu(\text{C}=\text{O})$, 1622 $\nu(\text{C}=\text{N})$ 1531, $\rho(\text{py})$ 646. Effective magnetic moment: 1.89 MB. UV–vis (DMSO, λ in nm/ ϵ in mol⁻¹dm²): 398/2.59 $\times 10^5$; 754/229. Yield 87 %

Dichloro(pyrazineformamide-isonicotinoyl hydrazone)copper(II), hydrate $[\text{Cu}(\text{HPzAmIH})\text{Cl}_2] \cdot 1.25\text{H}_2\text{O}$ (8)

Brown solid. Anal. Calc. for $\text{C}_{11}\text{H}_{12.25}\text{Cl}_2\text{CuN}_6\text{O}_{2.25}$ (FW = 394.70 g mol⁻¹): C, 33.09 %; H, 3.16 %; N, 21.05 %. Found: C, 33.27 %; H, 2.90 %; N, 20.66 %. IR (ATR, cm⁻¹): $\nu(\text{N}-\text{H})$ 3055, $\delta(\text{NH}_2)$ 1666, $\nu(\text{C}=\text{O})$ 1616, $\nu(\text{C}=\text{N})$ 1525, $\rho(\text{py})$ 654. Molar conductivity (1×10^{-3} mol L⁻¹ DMSO): 33.1 Ω^{-1} cm² mol⁻¹. Effective magnetic moment: 1.91 MB. UV–vis (DMSO, λ in nm/ ϵ in mol⁻¹dm²): 332/2.60 $\times 10^4$, 425/6.36 $\times 10^4$, 764/229. Yield 91 %.

Crystallography

Single-crystal X-ray diffraction methods were used to determine the structures of $[\text{Cu}(\text{HAPIH})\text{Cl}]\text{Cl} \cdot \text{H}_2\text{O}$ (6a) and $[\text{Cu}(\text{HPzAmIH})\text{Cl}_2] \cdot \text{H}_2\text{O}$ (8a). Data were

collected at room temperature on a Bruker D8 VENTURE equipped with Mo K α high-brilliance 1 μ S radiation ($\lambda = 0.71073 \text{ \AA}$) and a PHOTON 100 CMOS detector. The instrument was controlled by the APEX2 software package (Bruker 2014). Data were processed using the integrate plug-in in the controlling software package (SAINT) and corrected for absorption by the multiscan semi-empirical method implemented in SADABS (Bruker 2014). Using Olex2 (Dolomanov et al. 2009) the structure was solved with the SHELXS-97 (Sheldrick 2008) structure solution program by means of Direct Methods and refined with the SHELXL-2013 (Sheldrick 2008) refinement package using Least Squares minimization. Positional and anisotropic atomic displacement parameters were refined for all non-hydrogen atoms. Hydrogen atoms were placed geometrically and the positional parameters were refined using a riding model.

In vitro biological activity assays

Cytotoxicity toward human tumor cell lines

The cytotoxic activity of compounds **1–8** was tested against SF-295 (glioblastoma multiforme), HCT-116 (colon adenocarcinoma) and OVCAR-8 (ovarian cancer), from National Cancer Institute (Bethesda, MD, USA). The cells were maintained in RPMI 1640 medium supplemented with 10 % fetal bovine serum, 2 mM glutamine, 100 μ g/mL penicillin, and 100 μ g/mL streptomycin at 37 °C/5 % CO₂. Each compound was previously dissolved in DMSO (stock solution), whose final concentration in the RPMI culture medium was kept below 0.1 % (v/v). For initial cytotoxic activity evaluation, compounds **1–8** (5 μ g/mL) were incubated with SF-295, HCT-116 and OVCAR-8 cell lines, for 72 h. Cell viability was determined by dye reduction 3-(4,5-dimethyl-2-thiazole)-2,5-diphenyl-2H-tetrazole bromide (MTT) assay to yield the formazan, which is detected by electronic spectroscopy (Mosman 1983). Compounds that inhibited the proliferation in more than 50 % were selected for determination of the half maximal inhibitory concentration (IC₅₀). To this end, 5–0.009 μ g mL⁻¹ range for compound concentration was used. All experiments were performed in least three replicates per compound and results are shown as the average and 95 % confidence interval of three independent experiments.

Antitubercular activity

Antimycobacterial activities of compounds **1–8**, as well as isoniazid and copper(II) chloride, were assessed against *Mycobacterium tuberculosis* H₃₇Rv ATCC 27294 using the Micro plate Alamar Blue Assay (MABA) (Franzblau et al. 1998). This methodology is nontoxic, uses a thermally-stable reagent and shows good correlation with proportional and BACTEC radiometric methods (Tortoli et al. 2002; Kontos et al. 2004). The method is described as follows: 200 ml of sterile deionized water was added to all outer-perimeter wells of 96 sterile well plates (falcon, 3072: Becton–Dickinson, Lincoln Park, NJ) to minimize evaporation of the medium in the test wells during incubation. The 96 plates received 100 mL of the Middlebrook 7H9 broth (Difco laboratories, Detroit, MI, USA) and successive dilution of the compounds was performed directly on the plate. The final drug concentrations tested were 0.01–20.0 mg/mL. Plates were covered and sealed with parafilm and incubated at 37°C for 5 days. Twenty five milliliter of a freshly prepared 1:1 mixture of Alamar Blue (Accumed International, WestlakeOhio) reagent and 10 % tween 80 were then added to the plate and incubated for 24 h. A blue color in the well was interpreted as no bacterial growth, and a pink color was scored as growth. The minimal inhibition concentration (MIC) was defined as the lowest drug concentration, which prevents a color change from blue to pink.

Results and discussion

Formation of the copper(II) complexes

Microanalyses suggest the formation of [Cu(HPCIH)Cl₂] \cdot 0.4H₂O (**5**), [Cu(HAPIH)Cl₂] \cdot 1.25H₂O (**6**), [Cu(HPAmIH)Cl₂] \cdot H₂O (**7**) and [Cu(HPzAmIH)Cl₂] \cdot 1.25H₂O (**8**). For complexes **5** and **6**, the hydrazones coordinate as zwitterionic forms (based on infrared spectroscopy), whereas neutral ligands are attached to the metal center in **7** and **8**. Molar conductivities of **5–8** weren't determined in commonly used solvents (Geary 1971) due to its low solubility. Instead, molar conductivities were measured in DMSO whose values suggest the compounds behave as weak electrolytes in solution (Zianna et al. 2016). This behavior is probably

consequence of either the labile nature of chloro ligands or metal coordinating feature of the solvent. At room temperature, powdered samples of complexes display effective magnetic moments (μ_{eff}) in the 1.85–1.91 BM range, which is higher than the spin-only value. Such divergence, which is not quite uncommon in mononuclear copper(II) complexes, is due to mixing-in of some orbital angular momentum from the closely lying excited states via spin–orbit coupling (Bhattacharyya et al. 1996).

Infrared spectra

Absorptions observed between 1545 and 1557 cm^{-1} assigned to the $\nu(\text{C}=\text{N})$ in the IR spectra of free hydrazones (**1–4**) shift to 1523–1531 cm^{-1} in the spectra of the copper(II) complexes (**5–8**), suggesting coordination through azomethine nitrogen (Parrilha et al. 2014). Absorptions attributed to $\rho(\text{py})$ observed at 613–665 cm^{-1} for **1–4** exhibit pronounced shift in spectra of complexes **5–8** (644–654 cm^{-1}), suggesting the pyridine nitrogen coordination (Ferraz et al. 2013).

Bands attributed to $\nu(\text{N–H})$ of secondary amines are absent in the spectra of **5** and **6**. On the other hand, a fairly strong and very broad absorption attributed to the $\nu(\text{N}^+\text{–H})$ stretching vibration of the pyridinium group (Lessa et al. 2011) is observed around 2600 cm^{-1} . Moreover, the $\nu(\text{C}=\text{O})$ absorptions at 1665–1677 cm^{-1} in the spectra of the uncomplexed hydrazones disappear in those ones of complexes **5** and **6**, in agreement with coordination of an enolate oxygen (Mondal et al. 2013). Thus, for **5** and **6** the hydrazones are attached to copper(II) as zwitterionic species. Nonetheless, for complexes **7** and **8**,

$\nu(\text{C}=\text{O})$ vibrations are present at 1616–1622 cm^{-1} , which are shifted in relation to the free hydrazones, in accordance with coordination through a keto oxygen (Mishra and Sharma 2009).

Electronic spectra

The electronic absorption spectra of hydrazones (**1–4**) and their complexes (**5–8**) were recorded at room temperature using DMSO as the solvent. The absorption spectra of the ligands are characterized by one band and a shoulder or by two bands in the 297–377 nm region, which are assigned to $n \rightarrow \pi^*$ and $\pi \rightarrow \pi^*$ transitions of azomethine and the carbonyl groups (Cohen and Flavian 1967; Gegiou et al. 1996; Sorrell 1989). In the UV–vis spectra of **5–8** these absorptions are shifted. Also, the complexes show a single broad band centred in 743–764 nm, which is typical for d–d transition of Jahn–Teller distorted copper(II) complexes in square pyramidal geometries (Tabbi et al. 2013).

Structural study of [Cu(HAPIH)Cl]Cl·H₂O (**6a**) and [Cu(HPzAmIH)Cl₂]·H₂O (**8a**)

Crystal data and structure refinement for **6a** and **8a** are summarized in supplementary information (online resource). Selected bond distances and angles for **6a** and **8a** are shown in Table 1. Compounds **6a** and **8a** crystallized in the triclinic and monoclinic systems, respectively. ORTEP (Farrugia 1997) drawings (Figs. 2, 3) display the hydrazones tridentate to the metal ion through $\text{N}_{\text{azo}}\text{N}_{\text{arom}}\text{O}$ system for both complexes, giving

Table 1 Selected bond lengths (Å) and angles (°) for [Cu(HAPIH)Cl]Cl·H₂O (**6a**) and [Cu(HPzAmIH)Cl₂]·H₂O (**8a**)

	6a	8a		6a	8a
Cu1–N1	2.0241(16)	2.0801(17)	Cl1–Cu1–N1	99.28(5)	101.13(5)
Cu1–N2	1.9324(16)	1.9112(17)	Cl1–Cu1–N2	165.17(5)	121.09(6)
Cu1–O1	1.9992(14)	2.0136(15)	Cl1–Cu1–O1	100.19(4)	92.66(6)
Cu1–Cl1	2.2332(5)	2.4170(7)	Cl1–Cu1–Cl2	–	103.97(2)
Cu1–Cl2	–	2.3106(7)	Cl2–Cu1–N1	–	92.54(5)
C7–N2	1.289(2)	1.304(3)	Cl2–Cu1–N2	–	134.91(6)
N2–N3	1.375(2)	1.385(2)	Cl2–Cu1–O1	–	102.16(5)
N3–C8	1.320(2)	1.306(3)	N1–Cu1–N2	79.67(7)	78.18(7)
C8–O1	1.280(2)	1.288(2)	N1–Cu1–O1	158.90(6)	156.84(6)
			N2–Cu1–O1	79.42(6)	78.76(6)
			C2–C7–N2–N3	179.87(17)	–179.59(16)
			N2–N3–C8–O1	2.5(3)	1.3(3)

rise to two five-membered rings. Despite the similarities in ligand structures, metal ions adopt different coordination numbers and geometries, that is, **6a** shows a distorted square planar geometry, in which one chloride

is attached to the metal center, whereas **8a** is a pentacoordinated compound, in which two chloride ions complete its coordination. According to Addison and co-workers (1984), for distorted pentacoordinate structures,

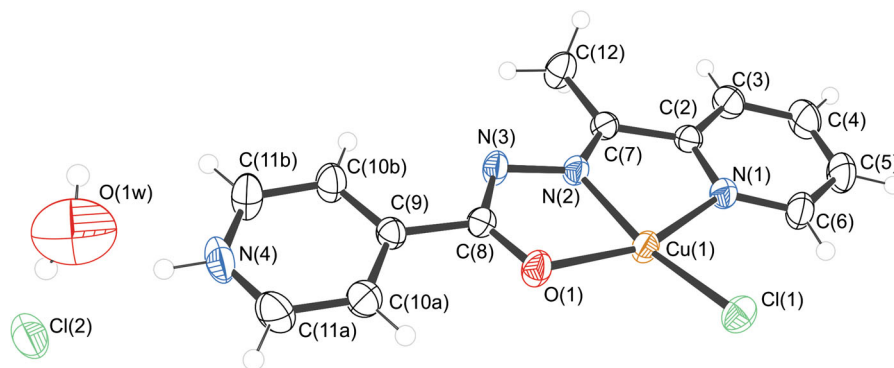


Fig. 2 ORTEP diagram for **6a** (ellipsoids at 50 % at probability)

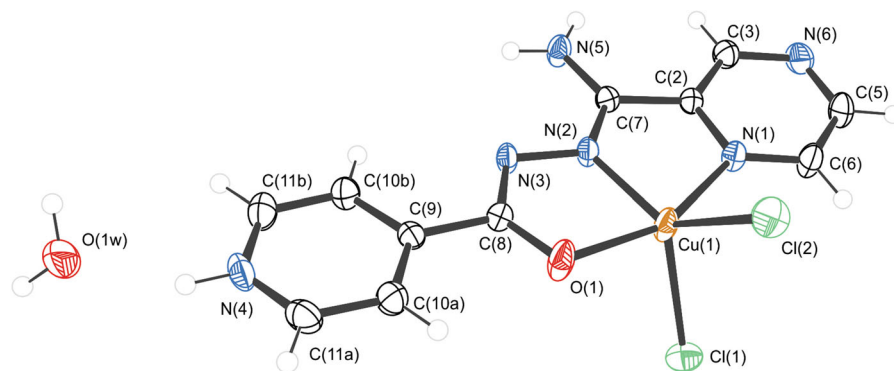


Fig. 3 ORTEP diagram for **8a** (ellipsoids at 50 % at probability)

Table 2 Hydrogen bond distances (Å) and angles (°) for [Cu(HAPIH)Cl]Cl·H₂O (**6a**) and [Cu(HPzAmIH)Cl₂]·H₂O (**8a**)

D—H...A	D—H	H...A	D...A	D—H...A
6a				
N4—H4...Cl2	0.86	2.23	3.057(2)	163
O1 W—H1 WA...Cl2	0.85	2.42	3.203(3)	154
O1 W—H1 WB...Cl2 ^a	0.85	2.56	3.341(3)	153
8a				
N4—H4...O1 W	0.86	2.00	2.746(3)	145
N5—H5A...Cl2 ^b	0.86	2.43	3.2575(18)	161
N5—H5B...Cl1 ^c	0.86	2.49	3.2098(18)	142
O1W—H1WA...Cl2 ^d	0.85	2.32	3.168(2)	174
O1W—H1WB...Cl1 ^e	0.85	2.55	3.2828(19)	146

Symmetry code: ^a $-x + 2, -y, -z + 2$; ^b $x + 1/2, -y + 1/2, z + 1/2$; ^c $-x + 1, -y, -z + 1$; ^d $-x + 1, -y + 1, -z + 1$; ^e $-x + 2, -y + 1, -z + 1$

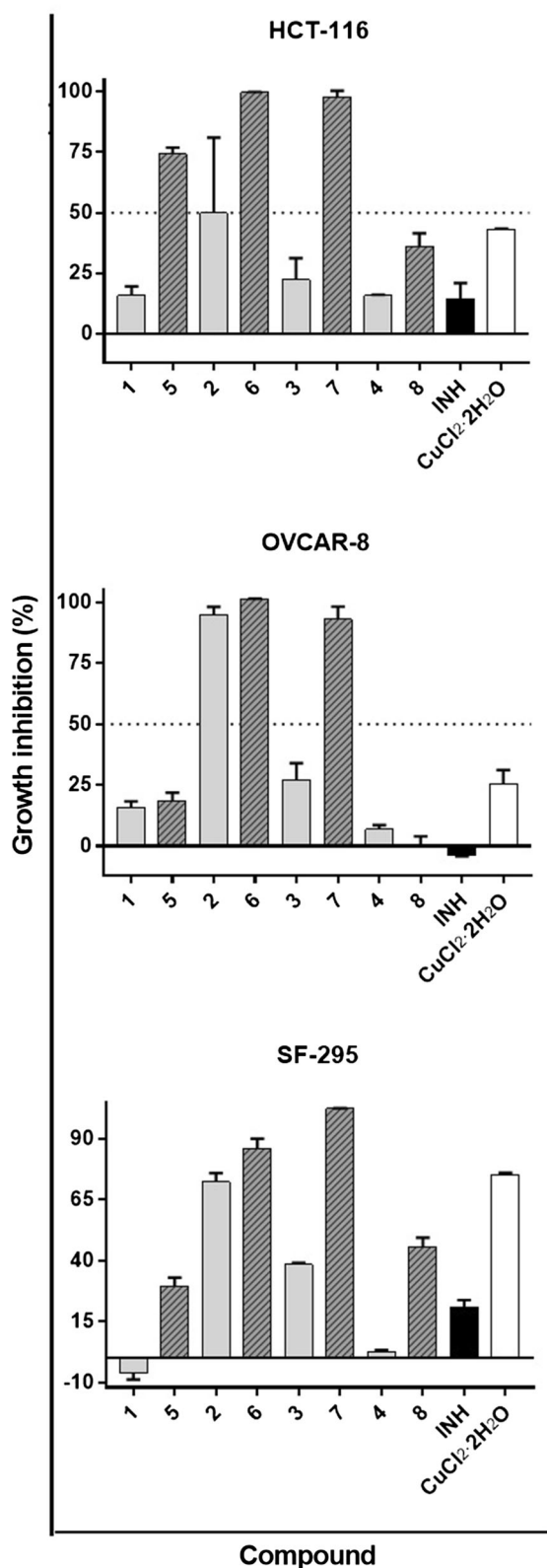


Fig. 4 Growth inhibition (GI, %) of OVCAR-8, HCT-116 and SF-295 cells promoted by **1–8**, copper(II) chloride and isoniazid (INH)

the parameter τ ($\tau = (\beta - \alpha)/60^\circ$, where α and β are the largest angles around the metal center) can be used to rationalize its geometries. Value τ is 0 for perfectly square-pyramidal geometry and 1 for perfectly trigonal-bipyramidal geometry. For **8a**, τ is 0.36, which suggests it is likely a distorted square-pyramidal compound.

Hydrazone ligands are nearly planar whose *rms* deviation of atoms from the least-squares plane is 0.0782 Å for **6a** and 0.0588 Å for **8a**. Metal ions lay close onto this plane (at 0.0481(10) and 0.0715(10) Å for **6a** and **8a**, respectively), as well as chlorine ligand in **6a** (0.638(2) Å).

The N3–C8 bond lengths 1.320(2) and 1.306(3) Å found for hydrazones in **6a** and **8a**, respectively, is shorter than the similar free hydrazone HBPIH (1.3601 (1) Å) (Ababei et al. 2010). Furthermore, C8–O1 bond is marked longer in **6a** (1.280(2) Å) and **8a** (1.288(2) Å) in comparison with HBPIH (1.2152 (1) Å). The C8–O1 bond is most likely to change from a double to a predominantly single bond and N3–C8 acquires some double bond character when hydrazones are attached to copper(II) in the enolate form (Despaigne et al. 2012; Mondal et al. 2013).

Besides, the enolate ligands are protonated at the *para*-substituted pyridine nitrogen in both complexes, indicating it is attached to the metal ion in the zwitterionic form. Complex **8a** is also protonated in the powder, whereas zwitterionic form of **6a** was obtained only through the crystallization process.

The dihedral angles C2–C7–N2–N3 and N2–N3–C8–O1 are 179.87(17) and 2.5(3), respectively, for **6a** as well as –179.59(16) and 1.8(3) respectively for **8**, which are in accordance with *EZ* conformation adopted by the hydrazones when attached to copper(II).

Interactions in crystal packing for **6a** and **8a** are described in Table 2. The interaction between Cu1 and C11^(1-x, 2-y, 1-z) (2.6375(6) Å) is the main contact in structure of compound **6a**, which results in the formation of a dimeric arrangement. Study of hydrogen bonds reveals a chain along the [1–2 1] direction. For compound **8a**, a three-dimensional hydrogen-bonding network is observed connecting water molecules and coordination compound (see supplementary information).

Table 3 Cytotoxic activity (IC₅₀) against SF-295, OVCAR-8 and HCT-116 cell lines of **2**, **6** and **7** in comparison with doxorubicin

Compound	IC ₅₀ (μmol L ⁻¹)		
	HCT-116	OVCAR-8	SF-295
HAPIH (2)	0.8216 (0.6621–1.0193)	0.7800 (0.7246–0.8828)	1.4413 (1.1317–1.8350)
[Cu(HAPIH)Cl ₂].1.25 H ₂ O(6)	0.3886 (0.3568–0.4232)	0.4843 (0.4123–0.5689)	0.8552 (0.6678–1.0952)
[Cu(HPAmIH)Cl ₂].H ₂ O(7)	9.3466 (7.7880–10.3337)	8.8617 (6.8652–11.4396)	7.9513 (7.0137–90102)
Doxorubicin	0.230 (0.165–0.313)	0.488 (0.313–0.561)	0.423 (0.350–0.460)

Data are expressed as IC₅₀ values and 95 % confidence interval, obtained by non-linear regression from three independent experiments performed in triplicate. Doxorubicin was used as control

Table 4 Minimal inhibitory concentration of **1–8**, copper(II) chloride and isoniazid (INH) against *M. tuberculosis* H₃₇Rv (ATCC 27294)

Compound	MIC (μmol L ⁻¹)
HPCIH(1)	13.79
[Cu(HPCIH)Cl ₂].0.4H ₂ O(5)	0.85
HAPIH(2)	2.60
[Cu(HAPIH)Cl ₂].1.25H ₂ O(6)	1.58
HPAmIH(3)	51.81
[Cu(HPAmIH)Cl ₂].H ₂ O(7)	63.50
HPzAmIH(4)	>412.81
[Cu(HPzAmIH)Cl ₂].1.25H ₂ O(8)	126.7
INH	2.27
CuCl ₂ .2H ₂ O	146.6

Cytotoxicity against tumor cell lines

Figure 4 reports growth inhibition of the human tumor cell lines OVCAR-8, SF-295 and HCT-116 induced by compounds **1–4** (Amim et al. 2016) and its complexes **5–8**. INH and copper chloride dihydrate were also tested for comparison.

According to results, isoniazid proved to be poorly effective against the three cell lines. Copper chloride, in turn, reduced in 75 % the SF-295 cells growth, whereas it presented moderate to low activity against the other cell lines.

All copper(II) complexes were more effective in reducing growth of HCT-116 and SF-295 cells than the respective free hydrazones. Coordination led to significant higher cytotoxicity of **7** to OVCAR-8 cells than hydrazone **3**. **2** as well as its complex **6** also strongly inhibited OVCAR-8 cells growth. It is

noteworthy that complexes **6** and **7** were able to inhibit the growth of all cell lines in more than 90 %.

The most potent compounds HAPIH (**2**), [Cu(HAPIH)Cl₂].1.25H₂O (**6**) and [Cu(HPAmIH)Cl₂].H₂O (**7**) were selected to determine the concentration which inhibits 50 % of cell growth (IC₅₀) (Table 3). Complex **6** was found to be the most active compound against all strains, whose activity is superior to the free hydrazone **2**. Besides, **6** is as potent as the anticancer drug doxorubicin. Thus, coordination of **2** to copper(II) was an efficient approach to obtain compound with improved action against tumor SF-295, OVCAR-8 and HCT-116 cell lines.

Antimycobacterial activity

Determined values of minimum inhibitory concentrations (MIC) of hydrazones **1–4**, their complexes **5–8**, INH and copper(II) chloride salt against *Mycobacterium tuberculosis* H₃₇Rv (ATCC 27294) are listed in Table 4.

Selected hydrazones display different behavior toward *M. tuberculosis*. HPCIH (**1**) shows moderate activity, whereas substitution of hydrogen at imine carbon by a methyl group in HAPIH (**2**) increases the antimycobacterial potency. HAPIH (MIC = 2.60 μM) is as effective as the reference antitubercular drug INH (MIC = 2.27 μM) in inhibit *M. tuberculosis*. Nonetheless, the presence of formamide in HPAmIH (**3**) as well as pyrazine substituent in HPzAmIH (**4**) leads to moderate and lost of action, respectively. In general, coordination of hydrazones to copper(II) promotes reduction in MIC values. [Cu(HPCIH)Cl₂].0.4H₂O (**5**), for example, exhibited sub-micromolar MIC value (0.85 μM) and was around 15-fold more effective than HPCIH (**1**) (13.79 μM) in inhibit growth of *M.*

tuberculosis. Complexes **5** and $[\text{Cu}(\text{HAPIH})\text{Cl}_2] \cdot 1.25\text{H}_2\text{O}$ (**6**) displayed high activity against *M. tuberculosis*, as compared with isoniazid, which suggests the compounds are attractive candidates as antitubercular drugs.

Conclusion

In this work, copper(II) complexes **5–8** were evaluated toward three tumor cell lines (OVCAR-8, SF-295 and HCT-116). In most cases, chelation with metals gave rise to enhancement of the ligands activity against the tested cells. **6** and **7** were appointed as lead cytotoxic complexes. Additionally, **6** has proved to be as effective as the anticancer drug doxorubicin. Further work will be needed to understand the mechanism whereby the complex disturbs cellular proliferation.

Upon coordination to copper(II), activity against *Mycobacterium tuberculosis* H₃₇Rv growth significantly improved except for **7**. Copper(II) chloride is poorly effective, suggesting the action is probably due to the complex per se. Coordination of HPCIH (**1**) to copper(II) was an efficient strategy to produce a compound (**5**) with improved antimycobacterial action. Complex **5** was also more active than isoniazid, suggesting it is a promising compound, which should be considered for further studies aiming to confirm its potential as novel antitubercular drug candidate.

Acknowledgments This work was supported by Conselho Nacional de Desenvolvimento Científico e Tecnológico (CNPq) and Fundação de Amparo à Pesquisa do Estado do Rio de Janeiro (FAPERJ). The authors express sincere thanks to the LDRX-UFF for the X-ray facilities and measurements.

References

Ababei LV, Kriza A, Musuc AM, Andronesu C, Rogoza EA (2010) Thermal behavior and spectroscopic studies of complexes of some divalent transitional metals with 2-benzoyl pyridilisonicotinoylhydrazone. *J Therm Anal Calorim* 101:987–996

Addison AW, Rao TN, Reedijk J, Rijn J, Verschoo GC (1984) Synthesis, structure, and spectroscopic properties of copper(II) compounds containing nitrogen-sulphur donor ligands; the Crystal and molecular structure of aqua[1,7-bis(*N*-methylbenzimidazol-2'-yl)-2,6-dithiaheptane]copper(II)perchlorate. *J Chem Soc, Dalton Trans* 7(7):1349–1356

Amim RS, Firmino GSS, Rego ACPD, Nery AL, Da-Silva SAG, Souza MVN, Pessoa C, Resende JALC, Figueroa-Villar JD,

Lessa JA (2016) Cytotoxicity and leishmanicidal activity of isoniazid-derived hydrazones and 2-pyrazineformamide thiosemicarbazones. *J Braz Chem Soc* 27:769–777

Armstrong CM, Bernhardt PV, Chin P, Richardson DR (2003) Structural variations and formation constants of first-row transition metal complexes of biologically active aroyl-hydrazones. *Eur J Inorg Chem* 6:1145–1156

Becker E, Richardson DR (1999) Development of novel aroyl-hydrazone ligands for iron chelation therapy: 2-Pyridyl-carboxaldehyde isonicotinoyl hydrazone analogs. *J Lab Clin Med* 134:510–521

Beraldo H, Gambino D (2004) The wide pharmacological versatility of semicarbazones, thiosemicarbazones and their metal complexes. *Mini-Rev Med Chem* 4:31–39

Bernardes-Génisson V, Deraeve C, Chollet A, Bernadou J, Pratiel G (2013) Isoniazid: an update on the multiple mechanisms for a singular action. *Curr Med Chem* 20(35):4370–4385

Bhattacharyya S, Kumar SB, Dutta SK, Tiekink ERT, Chaudhury M (1996) Zinc(II) and copper(II) complexes of pentacoordinating (N4S) ligands with flexible pyrazolyl arms: syntheses, structure, and redox and spectroscopic properties. *Inorg Chem* 35:1967–1973

Bruker (2014) APEX2, SAINT and SADABS. Bruker AXS Inc, Madison, Wisconsin

Chang H, Jia L, Xu J, Xu Z, Chen R, Wu W, Bie H, Zhu T, Ma T, Wang Y (2015) Syntheses, characterizations, antitumor activities and cell apoptosis induction of Cu(II), Zn(II) and Cd(II) complexes with hydrazone Schiff base derived from isonicotinohydrazone. *Inorg Chem Comm* 57:8–10

Chaves JDS, Damasceno JL, Paula MCF, de Oliveira PF, Azevedo GC, Matos RC, Lourenço MCS, Tavares DC, Silva H, Fontes APS, de Almeida MV (2015) Synthesis, characterization, cytotoxic and antitubercular activities of new gold(I) and gold(III) complexes containing ligands derived from carbohydrates. *Biometals* 28:845–860

Cohen MD, Flavian S (1967) Topochemistry. Part XXVI. The absorption spectra of some thermochromic *N*-salicylideneanilines and hydroxynaphthylideneanilines in the crystal. *J Chem Soc B* 317:329–334

Despaigne AAR, Da Costa FB, Piro OE, Castellano EE, Louro SRW, Beraldo H (2012) Complexation of 2-acetylpyridine- and 2-benzoylpyridine-derived hydrazones to copper(II) as an effective strategy for antimicrobial activity improvement. *Polyhedron* 38:285–290

Dheda K, Barry CE 3rd, Maartens G (2016) Tuberculosis. *Lancet* 387:1211–1226

Dolomanov OV, Bourhis LJ, Gildea RJ, Howard JAK, Puschmann H (2009) OLEX2: a complete structure solution, refinement and analysis program. *J Appl Cryst* 42:339–341

Ellis S, Kalinowski DS, Leotta L, Huang ML, Jelfs P, Sintchenko V, Richardson DR, Triccas JA (2014) Potent antimycobacterial activity of the pyridoxal isonicotinoyl hydrazone analog 2-pyridylcarboxaldehyde isonicotinoyl hydrazone: a lipophilic transport vehicle for isonicotinic acid hydrazide. *Mol Pharm* 85:269–278

Farrugia LJ (1997) ORTEP-3 for windows—a version of ORTEP-III with a graphical user interface (GUI). *J Appl Cryst* 30:565

Ferraz KSO, da Silva JG, Costa FM, Mendes BM, Rodrigues BL, dos Santos RG, Beraldo H (2013) N(4)-Tolyl-2-

- acetylpyridine thiosemicarbazones and their platinum(II, IV) and gold(III) complexes: cytotoxicity against human glioma cells and studies on the mode of action. *Biometals* 26:677–691
- Franzblau SG, Witzig RS, McLaughlin JC, Torres P, Madico G, Hernandez A, Degnan MT, Cook MB, Quenzer VK, Ferguson RM, Gilman RH (1998) Rapid, lowtechnology MIC determination with clinical *Mycobacterium tuberculosis* isolates by using the microplate Alamar blue assay. *J Clin Microbiol* 36:362–366
- Geary WJ (1971) The use of conductivity measurements in organic solvents for the characterization of coordination compounds. *Coord Chem Rev* 7:81–122
- Gegiou D, Lambi E, Hadjoudis E (1996) Solvatochromism in *N*-(2-Hydroxybenzylidene)aniline, *N*-(2-Hydroxybenzylidene)benzylamine, and *N*-(2-Hydroxybenzylidene)-2-phenylethylamine. *J Phys Chem* 100(45):17762–17765
- Glushkov RG, Modnikova GA, L'vov IA, Krylova LY, Pushkina TV, Gus'kova TA, Solov'eva NP (2004) Synthesis and antituberculosis activity in vitro and in vivo of novel amidine and hydrazidine analogs of pyrazinamide and isoniazid. *Pharm Chem J* 38:16–19
- Hearn MJ, Cynamon MH, Chen MF, Coppins R, Davis J, Joo-On Kang H, Noble A, Tu-Sekine B, Terrot MS, Trombino D, Thai M, Webster ER, Wilson R (2009) Preparation and antitubercular activities in vitro and in vivo of novel Schiff bases of isoniazid. *Eur J Med Chem* 44:4169–4178
- Hoagland DT, Liu J, Lee RB, Lee RE (2016) New agents for the treatment of drug-resistant *Mycobacterium tuberculosis*. *Adv Drug Del Rev* 102:55–72
- Judge V, Narasimhan B, Ahuja M (2012) Isoniazid: the magic molecule. *Med Chem Res* 21:3940–3957
- Kontos F, Maniati M, Costopoulos C, Gitti Z, Nicolaou S, Petinaki E, Anagnostou S, Tselentis I, Maniatis AN (2004) Evaluation of the fully automated Bactec MGIT 960 system for the susceptibility testing of *Mycobacterium tuberculosis* to first-line drugs: a multicenter study. *J Microbiol Methods* 56(2):291–294
- Kumar HSN, Parumasivam T, Jumaat F, Ibrahim P, Asmawi MZ, Sadikun A (2014) Synthesis and evaluation of isonicotinoyl hydrazone derivatives as antimycobacterial and anticancer agents. *Med Chem Res* 23(1):269–279
- Lessa JA, Guerra JC, Miranda LF, Romeiro CFD, Da Silva JG, Mendes IC, Speziali NL, Souza-Fagundes EM, Beraldo H (2011) Gold(I) complexes with thiosemicarbazones: cytotoxicity against human tumor cell lines and inhibition of thioredoxin reductase activity. *J Inorg Biochem* 105:1729–1739
- Lessa JA, Ferraz KSO, Guerra JC, de Miranda LF, Romeiro CFD, Souza-Fagundes EM, Barbeira PJS, Beraldo H (2012) Spectroscopic and electrochemical characterization of gold(I) and gold(III) complexes with glyoxaldehyde *bis*(thiosemicarbazones): cytotoxicity against human tumor cell lines and inhibition of thioredoxin reductase activity. *Biometals* 25:587–598
- Lessa JA, Soares MA, dos Santos RG, Mendes IC, Salum LB, Daghestani HN, Andricopulo AD, Day BW, Vogt A, Beraldo H (2013) Gallium(III) complexes with 2-acetylpyridine-derived thiosemicarbazones: antimicrobial and cytotoxic effects and investigation on the interactions with tubulin. *Biometals* 26:151–165
- Matei L, Bleotu C, Baciui I, Draghici C, Ionita P, Paun A, Chifiriu MC, Sbarcea A, Zarafu I (2013) Synthesis and bioevaluation of some new isoniazid derivatives. *Bioorg Med Chem* 21:5355–5361
- Mishra AP, Sharma N (2009) Synthesis, characterization, X-ray and thermal studies of some schiff base metal complexes. *J Ind Council Chem* 26(2):125–129
- Mondal S, Naskara S, Deya AK, Sinnb E, Eribalb C, Herronc SR, Chattopadhyaya K (2013) Mononuclear and binuclear Cu(II) complexes of some tridentate aroyl hydrazones. X-ray crystal structures of a mononuclear and a binuclear complex. *Inorg Chim Acta* 398:98–105
- Mosman T (1983) Rapid colorimetric assay for cellular growth and survival: application to proliferation and cytotoxicity assays. *J Immunol Methods* 65:55–63
- Oludina YN, Voloshina AD, Kulik MV, Zobov VV, Bukharov SV, Tagasheva RG, Nugumanova GN, Burilov AR, Kravchenko MA, Skornyakov SN, Rusinov GL (2014) Synthesis, toxicity, and antituberculosis activity of isoniazid derivatives containing sterically hindered phenols. *Pharm Chem J* 48:5–7
- Parrilha GL, Ferraz KSO, Lessa JA, de Oliveira KN, Ramos JP, Souza-Fagundes EM, Ott I, Beraldo H (2014) Metal complexes with 2-acetylpyridine-*N*(4)-ortho-chlorophenyl thiosemicarbazone: cytotoxicity and effect on the enzymatic activity of thioredoxin reductase and glutathione reductase. *Eur J Med Chem* 84:537–544
- Parumasivam T, Kumar HSN, Ibrahim P, Sadikun A, Mohamad S (2013) Anti-tuberculosis activity of lipophilic isoniazid derivatives and their interactions with first-line anti-tuberculosis drugs. *J Pharm Res* 7:313–317
- Prozorov AA, Zaichikova MV, Danilenko VN (2012) *Mycobacterium tuberculosis* mutants with multidrug resistance: history of origin, genetic and molecular mechanisms of resistance, and emerging challenges. *Rus J Gen* 48(1):1–14
- Raman N, Raja JD, Sakthivel A (2008) Design, synthesis, spectroscopic characterization, biological screening, and DNA nuclease activity of transition metal complexes derived from a tridentate Schiff base. *Russ J Coord Chem* 34:400–406
- Ramani AV, Monika A, Indira VL, Karyavardhi G, Venkatesh J, Jeankumar VU, Manjashetty TH, Yogeewari P, Sriram D (2012) Synthesis of highly potent novel anti-tubercular isoniazid analogues with preliminary pharmacokinetic evaluation. *Bioorg Med Chem Lett* 22:2764–2767
- Sheldrick GM (2008) A short history of SHELX. *Acta Crystallogr* 64:112–122
- Sorrell TN (1989) Synthetic models for binuclear copper proteins. *Tetrahedron* 54:10–12
- Sotgiu G, Ferrara G, Matteelli A et al (2009) Epidemiology and clinical management of XDRTB: a systematic review by TBNET. *Eur Respir J* 33(4):871–881
- Tabbì G, Giuffrida A, Bonomo RP (2013) Determination of formal redox potentials in aqueous solution of copper(II) complexes with ligands having nitrogen and oxygen donor atoms and comparison with their EPR and UV–Vis spectral features. *J Inorg Biochem* 128:137–145
- Tortoli E, Benedetti M, Fontanelle A, Simonetti MT (2002) Evaluation of automated BACTEC MGIT 960 system for testing susceptibility of *Mycobacterium tuberculosis* to four major antituberculous drugs: comparison with

- the radiometric bactec 460 tb method and the agar plate method of proportion. *J Clin Microbiol* 40(2):607–610
- WHO (2014) Global tuberculosis Report WHO. Geneva, Switzerland: World Health Organization. http://apps.who.int/iris/bitstream/10665/137094/1/9789241564809_eng.pdf. Accessed 01 Aug 2016
- Wong EB, Cohen KA, Bishai WR (2013) Rising to the challenge: new therapies for tuberculosis. *Trends Microbiol* 21(9):493–501
- Zianna A, Psomas G, Hatzidimitriou A, Lalia-Kantouri M (2016) Ni(II) complexes with 2,2-dipyridylamine and salicylaldehydes: synthesis, crystal structure and interaction with calf-thymus DNA and albumins. *J Inorg Biochem*. doi:10.1016/j.jinorgbio